Experiment on Multiple Fuel Supplies to Air Breathing Rocket Combustors

Nobuo Chinzei,* Goro Masuya,† Kenji Kudo,‡ Atsuo Murakami,‡ and Tomoyuki Komuro ‡
National Aerospace Laboratory, Kakuda, Miyagi, Japan

An experimental study on multiple fuel supplies to cylindrical subsonic mode combustors of air breathing rockets was made for the purpose of reducing combustor length. The experiment consisted of two parts, one in which all the fuel was supplied through a rocket with multiple nozzles and the other in which a portion of the fuel was directly fed into a secondary combustor with the rest being supplied through a rocket with a single nozzle. The results are compared with each other and with those of a reference experiment in which a rocket with a single nozzle without fuel injection was used. In the case with multiple nozzles, mixing and combustion efficiencies were higher than those in the reference experiment for the same combustor length. They collapse to a single curve against the combustor length nondimensionalized by the rocket nozzle exit diameter, except for the combustion efficiencies for unstable combustion. Increase of the injection mass flow rate makes mixing and combustion efficiencies rise, but it soon becomes less effective beyond a certain limit. Combustion instability observed in the reference case for long combustors is suppressed in both cases.

Nomenclature

A = cross-sectional area
C = mass concentration
D = combustor diameter
d_r = rocket nozzle exit diameter
f = mass flux density of concentration = ρuC
L = combustor length
m = mass flow rate
p = pressure
u = velocity in the axial direction
x = axial distance from the combustor inlet
α = local excess air ratio = local value of a ratio of air to that required for complete burning
ϵ_e = rocket nozzle expansion ratio
η = efficiency
ρ = density

Subscripts

0 = mean value obtained from measured flow rates or average value over the cross-sectional area
a = air
c = combustion or combustor
e = combustor exit
f = total fuel
gc = "generalized choking" state (see Ref. 13)
i = injection or injectant
m = mixing
min = minimum value
o = oxygen
r = rocket or rocket exhaust
s = secondary fuel
sb = secondary fuel burned in the combustor
sc = total combustible secondary fuel
t = rocket nozzle throat
w = wall

Received Sept. 25, 1985; revision received June 25, 1986.

*Chief, Solid Rocket Section.
†Senior Researcher.
‡Research Engineer, Solid Rocket Section.

Introduction

ROCKET engines, which have been used mainly for national projects such as launching satellites or spacecraft, are different in their objectives from air breathing engines used for commerical air transportation. In view of the success of the Space Shuttle and the coming era of the space station and the aerospace plane, the advanced propulsion engines that will be used in the future for transportation to low Earth orbits should be as fully reusable and cost effective as air breathing engines. Performance of rocket engines has been greatly improved as a result of intensive research and development over the past several decades; further significant improvement of these engines cannot be expected. The specific impulse of rocket engines is inherently lower than that of air breathing engines because the former consume the vehicle-contained oxidizer in combustion, while the latter utilize oxygen in the atmosphere for combustion. On the other hand, thrust to weight ratio of air breathers is generally lower than that of rocket engines because of structural complexity and lower combustion pressure. Because the oxidizer is taken from the atmosphere during flight, the performance of air breathers varies with flight conditions.

In order to make use of the advantages and to compensate for the deficiencies of both types of engines mentioned above, rocket/air breathing composite engines have been proposed as a means of propulsion for boosters of launch vehicles, and their excellent launch capabilities have been reported.[1-3] The technologies necessary for such composite engines, however, are still undeveloped as compared with those of rocket engines. Further efforts in various fields are necessary for practical application of such engines.

Air breathing rockets, shown in Fig. 1, are one type of rocket/air breathing composite engines and combine characteristics of rocket and ramjet engines. In the secondary combustor (referred to as a "combustor" hereafter) of air breathing rockets, fuel-rich hot exhaust from the primary rocket (referred to as a "rocket" hereafter) is mixed and reburned with air inhaled from the atmosphere to gain further thrust and thereby increase specific impulse. Fuel may be injected directly into the combustor if necessary. The present experiment was conducted to reduce the combustor length.

There have been numerous theoretical and experimental studies concerning mixing and combustion in air breathing rockets.[4-10] Hsia and Dunlap[6] showed that the theoretical performance derived from a one-dimensional analysis was

achieved at a length of five times the combustor diameter. Sosounov[7] correlated various experimental results for combustion efficiency by introducing the concept of "combustor equivalent length" and a correlation for a "diffusion flame length." He showed the possibility of reducing the combustor length by increasing the number of the rocket nozzles. Bendot[8] correlated lengths of ejectors with a parameter that included the number of primary nozzles, the mass flow rate ratio, and so on. Masuya et al.[10] have been studying mixing and combustion in air breathing rockets. They found that combustor length for sufficient performance varies with either rocket propellant oxidizer to fuel mixture ratio or air to rocket mass flow rate ratio.

In order to shorten the combustor, it is necessary to improve global mixing in the combustor. This can be accomplished by increasing the number of fuel supply points and by distributing them uniformly in the combustor before mixing between fuel from each fuel jet and the surrounding airstream begins. Needless to say, enhancing the mixing rate between fuel from a fuel jet and the air can improve global mixing as well as reduce combustor length. To investigate these effects, the present experiment consisted of two parts, one in which all the fuel was supplied through a rocket with multiple nozzles (multinozzle case), and the other in which a portion of the fuel was injected directly into the combustor with the rest being supplied through a rocket with a single nozzle (injection case). In our previous experiment,[10] it was found that an increase in either the rocket mixture ratio or air-rocket mass flow rate ratio could also improve mixing and combustion performance. The injection case implicitly includes these effects, too. The results are compared with those obtained in an experiment using a rocket with a single nozzle without fuel injection (reference case).

The experiment concerns so-called "subsonic mode combustion" where the flow is, on the average, subsonic in the combustor and thermally choked at the exit. Such a combustion mode is called "downstream choking mode" by Peters et al.[5] An experiment on "supersonic mode combustion" with a single nozzle without direct fuel injection was also conducted; results are reported in Ref. 9.

Experimental Apparatus

Schematics of the experimental apparatus for the multinozzle and the injection cases are shown in Figs. 2 and 3, respectively. The apparatus for the reference case is the same as that used in the injection case, except that the fuel injector was removed.

The rocket combustion chamber was made of copper, which allowed a burning time of 4.5 s without any active cooling. Ignition of the rocket was initiated by a spark plug located on the chamber wall. Expansion ratio and total throat area of the rocket nozzles were kept equal to those of the reference case, i.e., $\epsilon_e = 1.78$ and $A_t = 408$ mm^2. The combustor was a cylindrical stainless steel tube with an inner diameter of 100 mm. Its length L could be varied in 100 mm steps up to 1540 mm (multinozzle and reference cases) or 1570 mm (injection case). The difference of length is due to the injector section added in the latter case.

Propellants for the rocket were gaseous hydrogen and gaseous oxygen. The fuel for injection was also gaseous hydrogen, which was mixed with a small fraction (4%) of helium as a tracer to distinguish between the injected and the rocket supplied fuels. Air was fed from a high pressure reservoir at room temperature through a pressure regulator and a choked orifice so that the air flow rate was kept constant, independent of conditions in the combustor. In order to make comparisons among the three cases, the flow rates of air, oxygen, and total fuel were kept equal in all the cases at values of $m_a = 1.1$ kg/s, $m_o = 0.160$ kg/s, and $m_f = 0.048$ kg/s. The total hydrogen included the fuel for injection as well as that for the rocket. Mass flow rate of the fuel for secondary combustion (secondary fuel) m_s was 0.028 kg/s, which included injected fuel and excess hydrogen in the rocket exhaust. The total propellant oxidizer to fuel mixture ratio was 3:3; the ratio of air to total propellant mass flow ratio was 5:3; and the overall excess air ratio (the ratio of the air mass flow rate to that required for complete burning with the secondary fuel) was 1:13. The rocket combustion pressure was 1.2 MPa for the reference and the multinozzle cases. In the injection case, it decreased as injection mass flow rate, m_i, increased. These experimental conditions also resulted in an increase of the rocket mixture ratio and a reduction of the rocket mass flow rate with the increase in m_i.

In the multinozzle case, exhaust gas from the rocket was discharged through four or seven nozzles. Because the rocket propellant mass flow rate and the nozzle expansion ratio were kept equal to those in the reference case, diameters of throat and exit of the nozzles were inversely proportional to the square root of the number of the nozzles. The nozzles were distributed uniformly over the cross section of the combustor. They were made of graphite to prevent thermal load and were inserted into stainless steel sheaths for reinforcement.

In the injection case, the nozzle, which was also used in the reference case, was made of copper. Eighteen injection holes, each with a diameter of 2 mm and equally spaced circumferentially, were drilled normal to the combustor wall. Length of the injector section installed with these injection holes was 30 mm, resulting in a combustor length not exactly the same as that in the other cases. Most of the experiments concerned axial distances from the combustor inlet to the injection point, x_i, of 155 mm. A few experiments were conducted for distances shorter or longer than the above value. The results, however, are not included here because unstable combustion was experienced except for $x_i = 255$ mm. Results of the latter will be described briefly.

Data were taken after flow rates, combustion pressure, etc. became steady. Flow rates of air and propellants were

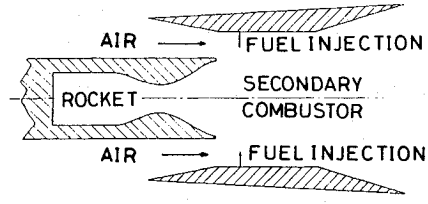

Fig. 1 Air breathing rockets.

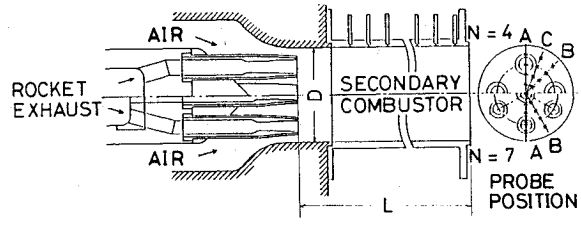

Fig. 2 Experimental apparatus (multinozzle case).

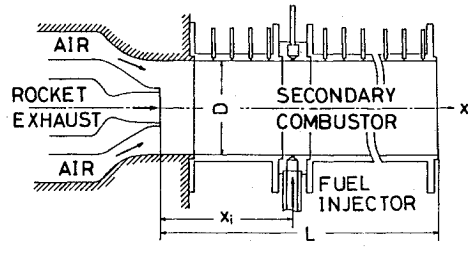

Fig. 3 Experimental apparatus (injection case).

measured by orifice flow meters. The flow rate of the tracer was determined by gas chromatographic analysis of a sample taken from the injector settling chamber. Pressure taps were installed every 20 mm in the axial direction on the wall. A water-cooled eleven-point probe rake was attached to the exit of the combustor to measure Pitot pressures and to draw gas samples. The samples were held in bottles and analyzed later with a gas chromatograph. The probes were located linearly and equally spaced in the radial direction. In order to obtain cross-sectional distributions in the multinozzle case, the probe measurements were made at two or three different positions, shown in Fig. 2, for each combustor length. In the injection case, circumferential variation of the distribution was not observed for the present experimental setup. The probe rake was removed when measuring wall pressures.

Results and Discussion

Wall Pressure Distributions

Wall pressure, p_w, is plotted as a function of axial distance, x, of the combustor with various lengths shown in Figs. 4 and 5 for the multinozzle and the injection cases, respectively. Distributions from the reference case are also shown in the figures. In Fig. 4, the axial distance is nondimensionalized by the rocket nozzle exit diameter, d_r. The exit wall pressures obtained by extrapolation are shown in the figures as symbol "X." In a "subsonic mode combustion" such as that in the present experiment, wall pressure generally decreases downstream as a result of heat addition produced by the combustion of the fuel with air. Wall pressures decrease with a frictional effect, too. For combustors long enough to allow complete mixing and combustion, distributions are almost the same except near the exit where the frictional effect would be dominant. This condition can be attained in the multinozzle case for combustor lengths greater than $30d_r$, as can be seen in Fig. 4. For L/d_r less than 30, wall pressures are lower than those in the longer combustors because of incomplete mixing and combustion.

In the injection case, the length necessary for sufficient combustion performance is around 600 mm (corresponding to $20d_r$), as can be seen in Fig. 5. The pressure distributions differ quite markedly from those in the multinozzle and the reference cases. Compared with the latter cases, a region of high pressure appears upstream of the injection holes and there is a region of steep negative pressure gradient just downstream. Consider the reference and the injection cases with the same degree of mixing and burning at the exit. In the present experiment, all the mass flow rates supplied to the combustor were kept constant. The stream thrust at the exit $(p_e + \rho_e u_e^2)A_e$, should be equal for both cases because the flow is choked there. Because the combustor cross-sectional area is constant, the stream thrust at the combustor inlet is equal to the sum of that at the exit and a friction force acting at the wall. Fuel injection would result in a decrease of rocket thrust because total hydrogen flow rate was kept constant. Thus in the injection case, the stream thrust of the air at the combustor inlet increases to make up for the deficient rocket thrust, leading to the pressure rise upstream of the injection (see Fig. 5). Therefore, it should be noted that higher ram pressure is required to operate air breathing rockets utilizing this type of fuel supply than those utilizing rocket-supplied fuel only. The steep negative pressure gradient immediately downstream corresponds to a large heat release, implying that mixing and combustion are remarkably enhanced by injection. Although not shown in Fig. 5, an increase in x_i from 155 to 255 mm causes the region of high pressure and the steep negative pressure gradient to move downstream accordingly.

Mass Concentration in the Combustor

Mass concentrations of the rocket exhaust C_r and injected fuel C_i were obtained from gas chromatographic analysis of samples drawn through the probes. Radial distribution of

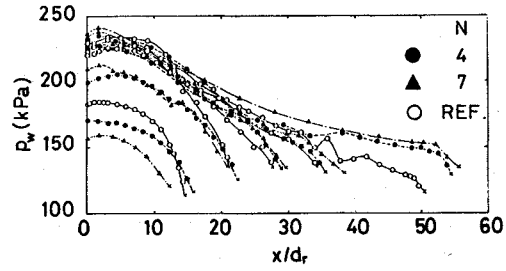

Fig. 4 Wall pressure distributions (multinozzle case).

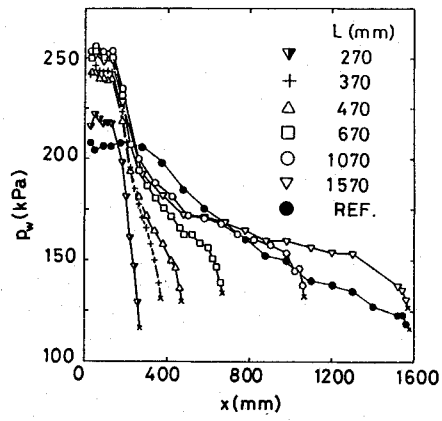

Fig. 5 Wall pressure distributions (injection case).

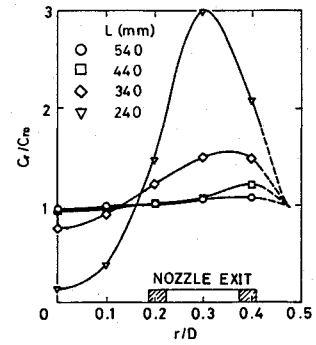

a) $N=4$.

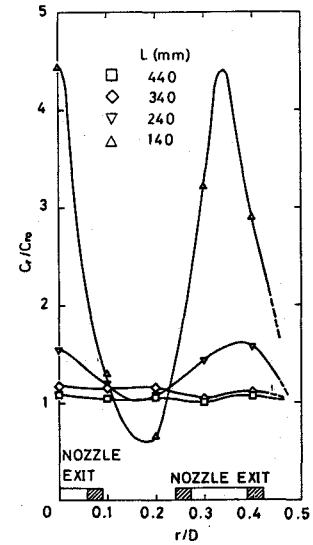

b) $N=7$.

Fig. 6 Radial distributions of rocket exhaust concentration (multinozzle case).

these concentrations will be presented by averaging the data of two points of equal distance from the center line and by normalizing them with their mean values (subscript "0") obtained from the measured flow rates. The radial distances are nondimensionalized by the combustor diameter, D.

Multinozzle Case

Radial distributions of C_r at the combustor exit are shown in Figs. 6a and 6b for the combustors with four and seven nozzles, respectively. The distributions are along the rake position "A" (see Fig. 2). As was expected, distribution for the combustor with seven nozzles becomes flat more rapidly than that with four nozzles. As combustor length increases, distributions become flat, approaching unity, and a distribution's maximum point moves toward the wall. The latter result is contrary to that of the experiment on nonreacting multiple free jets,[11] where the maximum point moved inward, tending to form a single free jet downstream. This difference would be mainly attributed to the presence of the combustor wall in the present case.[12]

Injection Case

Figures 7 and 8 show variations of radial distributions of C_i and C_r at the combustor exit with injection flow ratio m_i/m_f. With increasing injection flow ratio, distributions become flat. However, the effect of injection becomes less effective for a m_i/m_f beyond 0.25. These results will be discussed later, together with the results on combustor performance. When increasing x_i form 155 to 255 mm for fixed combustor length, the distribution of C_r becomes less uniform, but that of C_r remains almost unchanged.

In Fig. 9, axial distributions of C_i along the center line and on the combustor wall are shown. Note that the former is obtained from cross-sectional distributions at the exit of the combustor with different lengths, whereas the latter is for a single run with the longest combustor (1570 mm). Therefore, the comparison between the distributions is only qualitative. The concentration C_i/C_{i0} on the center line monotonously increases downstream and approaches unity, whereas that on the wall at first rapidly increases and overshoots above unity, then decreases toward the value on the center line.

Combustor Performances

In the multinozzle and the reference cases, combustor performance is mainly governed by mixing between the rocket and the air. In the injection case, on the other hand, the performance is also associated with mixing the injected fuel. Therefore, a mixing efficiency common to all the cases is defined as a measure of mixing the secondary fuel.

The mixing efficiency, η_m, thus defined is expressed as

$$\eta_m = 1 - \sqrt{\beta/\beta_{gc}} \tag{1}$$

$$\beta = \int_{A_e} \left(\frac{f_s}{f_{s0}-1}\right)^2 \frac{\mathrm{d}}{A_e} \tag{2}$$

where subscript 0 refers to the average values over the cross-sectional area. Subscript gc corresponds to a state of "generalized choking," defined in Ref. 13, where the flow is choked at the exit without any mixing and burning in the combustor. In order to account for mixing of either the rocket exhaust or the injected fuel only, the other two kinds of mixing efficiencies, η_{mr} and η_{mi}, are also defined. They are expressed by simply replacing f_s in Eq. (2) with f_r or f_i.

The combustion efficiency, η_c, is defined as the ratio of burned to total combustible secondary fuel, m_{sc} in the combustor,

$$\eta_c = \int_{Ae} f_{sb} \frac{\mathrm{d}A}{m_{sc}} \tag{3}$$

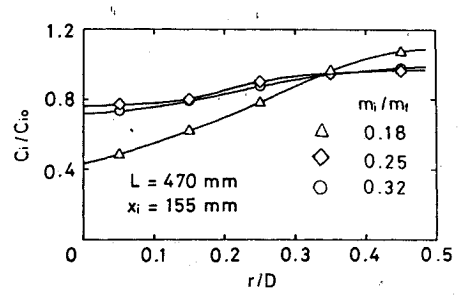

Fig. 7 Radial distributions of injectant concentration.

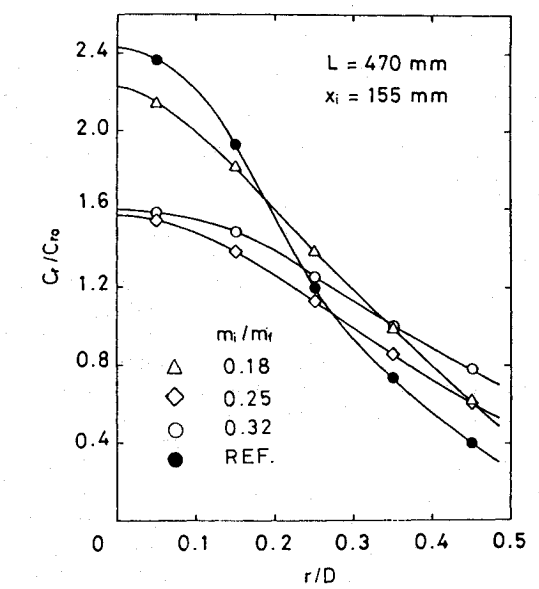

Fig. 8 Radial distributions of rocket exhaust concentration (injection case).

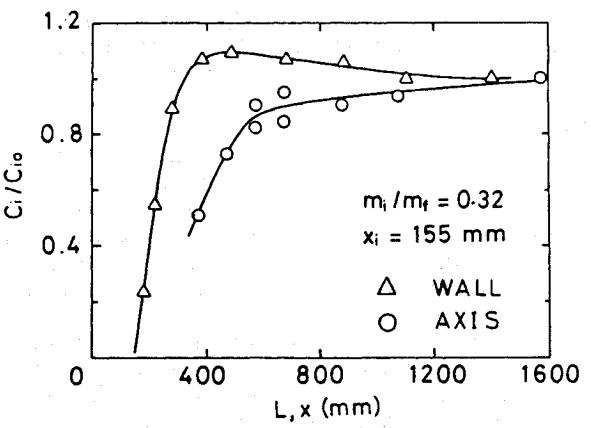

Fig. 9 Axial distribution of injectant concentration on the wall and the center line of the combustor.

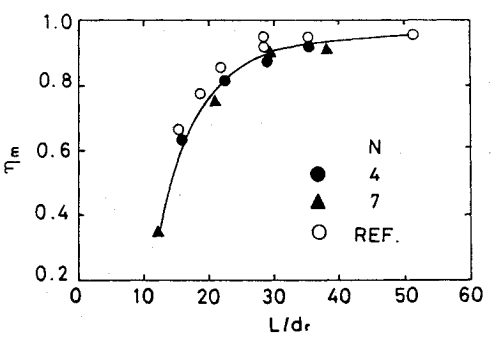

Fig. 10 Effect of the number of nozzles on mixing.

It should be noted that while the mixing efficiency defined in Eqs. (1) and (2) represents the uniformity of the secondary fuel distribution, it does not show the degree of mixing required for complete combustion. An efficiency indicating the latter, which will be shown and discussed later in more detail, is generally higher than η_m. Under the present experimental conditions, however, both are almost the same because the overall mixture ratio is nearly stoichiometric. The integrations appearing in Eqs. (2) and (3) are carried out over the exit cross section. All the quantities included in the preceding equations can be obtained from measured mass flow rates, Pitot pressure, and gas sampling data.

Multinozzle Case

Variations of the mixing and combustion efficiencies with the combustor length are shown in Figs. 10 and 11, together with those of the reference case. The combustor length is nondimensionalized by d_r. The efficiencies increase with combustor length. The mixing efficiencies collapse to a single curve irrespective of the number of nozzles. As the rocket propellant mass flow rate and the nozzle expansion ratio were kept equal to those in the reference case, this indicates that the flowfield produced by each nozzle is similar to that in the reference case. The combustor length for sufficient mixing is again $30d_r$, inversely proportional to the square root of the number of the nozzles. The global mixing improvement in this case is solely due to the effect of distributing fuel supply points uniformly over the combustor cross section.

The combustion efficiencies also collapse to a single curve against the same nondimensional combustor length, except in the reference case, as can be seen in Fig. 11. In the latter case with long combustors, low frequency noise, pressure fluctuations in the air stream, or unusual wall pressure distributions were observed. They are considered as symptoms of combustion instability resulting in lower combustion efficiency. Therefore, increasing the number of the rocket nozzles tends to suppress the combustion instability as well as improve global mixing and combustion. Except for those unstable conditions, the same conclusions regarding the effect of the number of the nozzles as those on the mixing efficiency can be made.

Injection Case

Variations of the mixing and the combustion efficiencies with injection mass flow rate for a combustor length of 470 mm are shown in Figs. 12 and 13. The other two types of mixing efficiencies, η_{mr} and η_{mi}, are also shown in Fig. 12. All the efficiencies increase with an increase in injection mass flow rate. The improvement in global mixing seen in this case is due to two previously mentioned effects: distributing fuel supply points uniformly over the cross section, and enhancing diffusion of each fuel jet and the rocket exhaust. The value of η_{mi} is near unity, showing that the injected fuel is diffused more rapidly than the rocket exhaust because of the smaller diameter of injection holes as compared with that of the rocket nozzle exit.

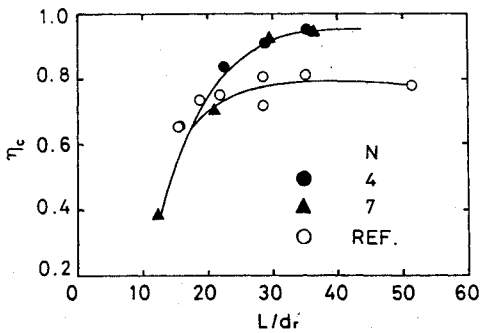

Fig. 11 Effect of the number of nozzles on combustion.

As observed previously in Fig. 8, which shows the cross-sectional distributions, η_{mr} is insensitive to injection mass flow rate for the larger value of m_i/m_f. Such an effect may be due to the following reasons: 1) turbulence produced in the surrounding stream by injected fuel jets may enhance mixing of the fuel jets and the rocket exhaust, but it was found[14] that the effect reaches an upper limit for turbulence beyond a certain level; 2) as stated in the previous work,[10] an increase in the rocket mixture ratio can improve mixing of the rocket exhaust, but it also becomes less effective when further increased.

Variations of mixing efficiencies and combustion efficiency with combustor length are shown in Figs. 14 and 15, respectively; they increase with an increase in combustor length. Even for short combustors, they are much higher than those in the reference case. Within the range of combustor lengths tested, η_{mi} is again near unity, indicating a rapid diffusion of

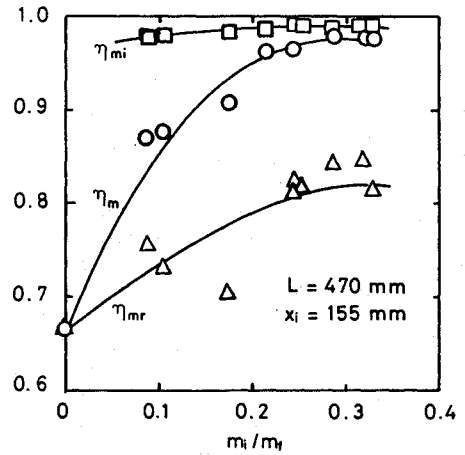

Fig. 12 Effect of injection mass flow rate on mixing.

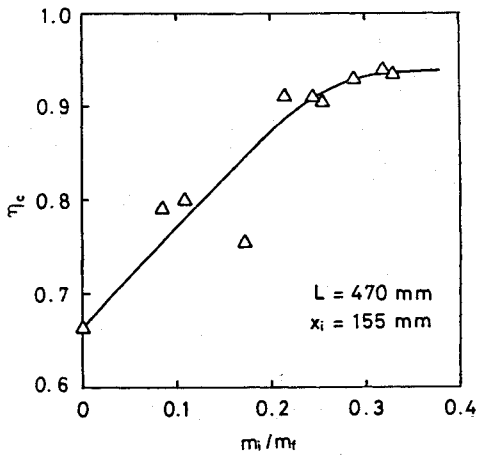

Fig. 13 Effect of injection mass flow rate on combustion.

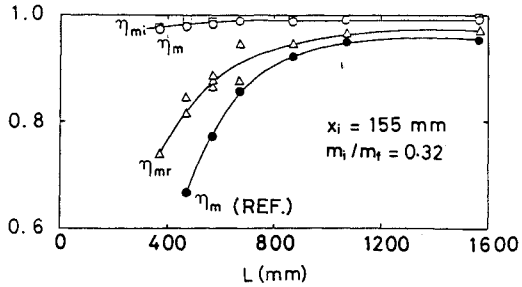

Fig. 14 Effect of combustor length on mixing (injection case).

the fuel jets. By decreasing combustor lengths beyond those indicated in the figure, however, η_{mi} may steeply decrease toward zero, as implied in Fig. 9. By comparing Fig. 14 with Fig. 15, it can be seen that the effect of injection on η_m directly corresponds to that on η_c for short combustors. For long combustors, however, the effect of injection on η_c is much greater than that on η_m, as in the multinozzle case. This can again be considered as a result of the combustion stabilization made by injection. In order to provide η_c for a hypothetical reference case without combustion instability, a correction is made by use of the multinozzle data. The hypothetical reference data are assumed to be on the collapsed curve in Fig. 11. They are shown in Fig. 15 by a broken curve. By using this correction, correspondence between η_m and η_c can be extended to long combustors.

The effect of axial injection location, x_i, on combustor performance cannot be clarified because of the limited results. However, there is an optimum range for the injection location $x_i = 155 \sim 255$ mm. Outside this range, unstable combustion was observed, which resulted in lower η_c.

As can be expected from the fact that fuel injection improves the mixing of the rocket exhaust, the presence of the rocket exhaust stream may improve diffusion of the fuel jets. Figure 16 shows variations of a mixing parameter of the injectant with distance from the injector to the exit for cases with and without the rocket operation. In the latter case, combustion did not occur. The mixing efficiency of the injected fuel, η_m, is not used as a measure of mixing because it cannot be obtained in the case without the rocket operation due to the unchoked exit state. The minimum concentration of the injected fuel on the exit section, $C_{i\,\min}$, is used here. This parameter emphasizes the effect of the rocket operation because η_{mi} is near unity and shows little variation in the present experiment. By operating the rocket, $C_{i,\min}/C_{i0}$ and its rate of change with distance are increased. These results may be due to the turbulence effect of greater velocity and length scales produced by the rocket exhaust stream as compared with those produced by the fuel jets alone.

As implied in the previous discussion, there seems to be a correlation between mixing and combustion, which is shown in Figs. 17a and 17b. In Fig. 17a, η_c is plotted against previously defined η_m. In the multinozzle and the reference cases, η_c and η_m correlate well, except in the latter case for η_m near unity, where unstable combustion was observed. In the injection case, however, η_c is somewhat higher than η_m and does not agree with those in the other cases. In order to see whether or not this disagreement is the result of a difference in the combustion mechanisms, we introduce another type of mixing efficiency that is related more directly to the combustion. The new mixing efficiency, η_{mc}, is defined as

$$\eta_{mc} = \int_{Ae} \rho u C' \frac{dA}{m_{fc}} \tag{4}$$

where

$$C' = C_s \quad (\alpha > 1) \tag{5}$$

or

$$C' = \alpha C_s / (\alpha < 1) \tag{6}$$

and α is a local excess air ratio. The relation between η_{mc} and η_c is shown in Fig. 17b. The disagreement between the multinozzle and the injection cases that appeared in Fig. 17a is not seen in Fig. 17b. Thus the combustion is controlled

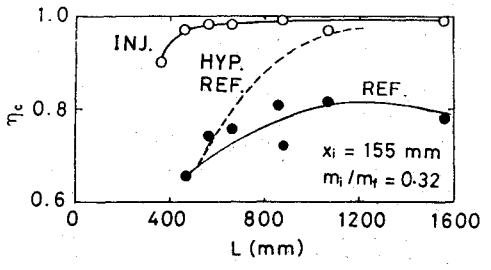

Fig. 15 Effect of combustor length on combustion (injection case).

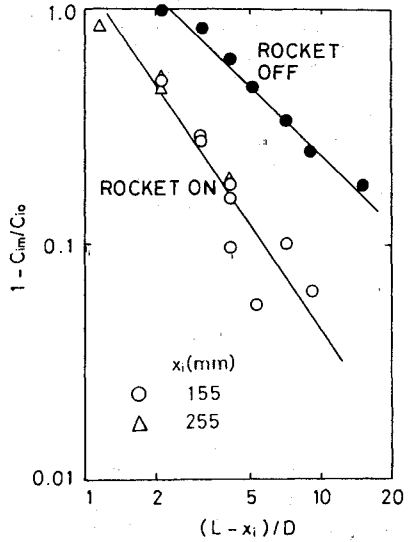

Fig. 16 Effect of rocket operation on mixing of injectant.

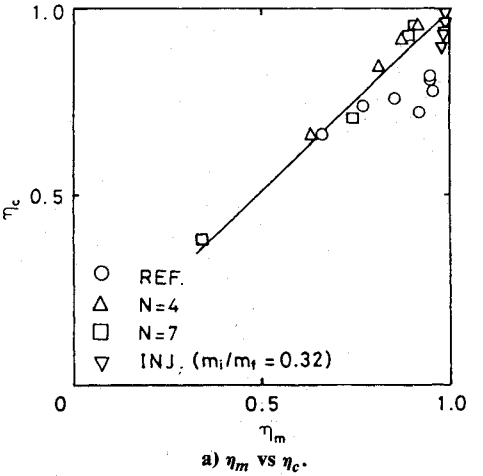

a) η_m vs η_c.

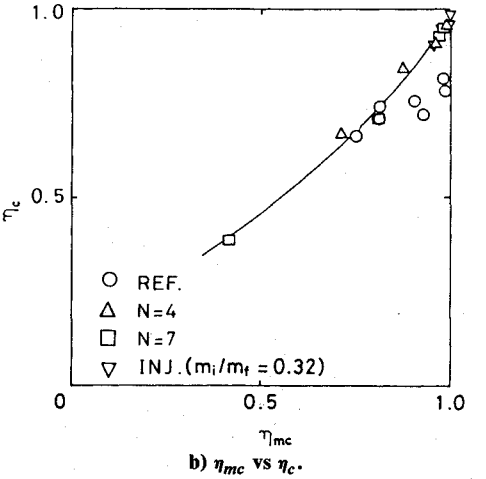

b) η_{mc} vs η_c.

Fig. 17 Correlation between mixing and combustion.

mainly by global mixing in all the cases irrespective of the type of fuel supply.

Conclusions

Experimental results on the multiple fuel supplies to the secondary combustor of air breathing rockets have been presented. The experiment consisted of two parts: one in which all the fuel was supplied through a rocket with multiple nozzles; and the other in which a portion of the fuel was directly injected into the secondary combustor while the rest was supplied through a rocket with a single nozzle. The results are compared with each other and with that of a reference experiment in which fuel was supplied only through a rocket with a single nozzle. They are summarized as follows:

1) Performance of mixing and combustion in the secondary combustors is improved in both cases.

2) Combustion instability, which has been observed in the reference experiment with long combustors, is suppressed.

3) In the experiment using a rocket with multiple nozzles, the combustor length required for sufficient performance of mixing and combustion is inversely proportional to the number of nozzles, except for the combustion efficiencies for the previously mentioned unstable conditions in the reference case. This effect is due to distributing the fuel supply points uniformly over the combustor cross section.

4) The effect of injection is not only to distribute the fuel supply points uniformly over the combustor cross section but also to improve diffusion of fuel jets and the rocket exhaust. The latter effect is due to turbulence produced by the fuel jet and the increase in the rocket mixture ratio.

5) If the injection mass flow rate is increased beyond a certain limit, the mixing and combustion efficiencies become less sensitive to the injection mass flow rate.

6) Mixing of injected fuel is enhanced by the presence of the rocket exhaust stream.

7) There is a correlation between mixing and combustion irrespective of the type of fuel supply, except for the previously mentioned unstable conditions in the reference case.

8) It appears possible to shorten the combustor to any desired length by simply increasing the number of nozzles. However, the rocket with multiple nozzles is difficult to manufacture and there could be serious heating and structural load problems, expecially on the nozzles and the branching section extending from the rocket combustion chamber to the nozzles. When provided with sufficient ram pressure, therefore, supplying fuel by injection would be preferable for practical purposes.

Acknowledgment

The authors wish to express their gratitude to Mr. Shinichi Ishii, the former chief of the Solid Rocket Section, who conducted the present work with the authors.

References

[1]Larson, V. R., "Future Propulsion Option for Performance Growth," AIAA Paper 76-708, July 1976.

[2]Kramer, P. A. and Buehler, R. D., "Hybrid Rocket/Airbreathing Propulsion for Ballistic Space Transportation," *Journal of Spacecraft and Rockets,* Vol. 17, July-Aug. 1980, pp. 334-341.

[3]Chase, R. L., "A Comparative Assessment of Priority Launch Vehicle Concepts," AIAA Paper 80-1131, June 1980.

[4]Perini, L. L., Wilson, W. E., Walker, R. E., and Dugger, G. L., "Preliminary Study of Air Augmentation of Rocket Thrust," *Journal of Spacecraft and Rockets,* Vol. 1, Nov.-Dec. 1964, pp. 626-634.

[5]Peters, C. E., Phares, W. J., and Cunningham, T.H.M., "Theoretical and Experimental Studies of Ducted Mixing and Burning of Coaxial Streams," *Journal of Spacecraft and Rockets,* Vol. 6, Dec. 1969, pp. 1435-1441.

[6]Hsia, H. T. S., Dunlap, R., "A Parametric Study of Secondary Combustion," *Astronautica Acta,* Vol. 16, March 1971, pp. 127-135.

[7]Sosounov, V. A., "Some Problems Concerning Optimal Ducted Rocket Engine," *Proceedings of the 2nd International Symposium on Air Breathing Engines*, The Royal Aeronautical Society, Sheffield, England, March, 1974.

[8]Bendot, J. G., "Hypermixing Ejectors for Composite Engines," *Proceedings of the 3rd International Symposium on Air Breathing Engines,* Deutsche Gesellschaft fur Luft-und Raumfahrt, Munich, FRG, March 1976, pp. 925-940.

[9]Masuya, G., Ishii, S., Kudo, K., Murakami, A., and Komuro, T., "A Study of Air Breathing Rockets (4) — Supersonic Mode Combustion," *Proceedings of Seventeenth Symposium (Japan Section) on Combustion*, The Combustion Institute Japan Section, Nagoya, Japan, Dec. 1979, pp. 96-98.

[10]Masuya, G., Chinzei, N., and Ishii, S., "A Study of Air Breathing Rockets—Subsonic Mode Combustion," *Acta Astronautica*, Vol. 8, May-June 1981, pp. 643-661.

[11]Raghunathan, S. and Reid, I. M., "A Study of Multiple Jets," *AIAA Journal*, Vol. 19, Jan. 1981, pp. 124-127.

[12]Okamoto, T., Yagita, M., Watanabe, A., and Kawamura, K., "Interaction of Twin Turbulent Circular Jets," *Transactions of the Japan Society of Mechanical Engineers,* Series B, Vol. 50, No 456, 1984 (in Japanese).

[13]Hoge, H. J. and Segars, R. A., "Choked Flows: A Generalization of the Concept and Some Experimental Data," *AIAA Journal*, Vol. 3, March 1965, pp. 2177-2183.

[14]Goldschmidt, V. W., "Open Forum," *Proceedings of the Conference on Free Turbulent Shear Flows*, NASA SP-321, pp. 637-639, 1972.